In situ X-ray Rietveld analysis of Ni–YSZ solid oxide fuel cell anodes during NiO reduction in H_2

A. Reyes-Rojas, H.E. Esparza-Ponce, L. Fuentes, A. Lòpez-Ortiz, A. Keer and J. Reyes-Gasga.

Abstract

A synthesis and characterization of solid oxide fuel cell (SOFC) anodes of nickel with 8%mol yttrium stabilized zirconia (Ni–YSZ) is presented. Attention was focused on the kinetics and phase composition associated with the transformation of NiO–YSZ to Ni–YSZ. The anodes were prepared with an alternative synthesis method that includes the use of nickel acetylacetonate as an inorganic precursor to obtain a highly porous material after sintering at 1400°C and oxide reduction (NiO–YSZ→Ni–YSZ) at 800°C for 8 h in a tubular reactor furnace using 10% H_2/N_2. The obtained material was compressed by unidirectional axial pressing into 1 cm-diameter discs with 15–66 wt% Ni and calcinated from room temperature to 800°C. A heating rate of 1°C min^{-1} showed the best results to avoid any anode cracking. Their structural and chemical characterization during the isothermal reduction were carried out by in situ time-resolved X-ray diffraction, refined with the Rietveld method (which allowed knowing the kinetic process of the reduction), scanning electron microscopy and X-ray energy dispersive spectroscopy. The results showed the formation of tetragonal YSZ 8%mol in the presence of nickel, a decrement in the unit cell volume of Ni and an increment of Ni in the Ni–YSZ anodes during the temperature reduction. The analysis indicated that the Johnson–Mehl–Avrami equation is unable to provide a good fit to the kinetics of the phase transformation. Instead, an alternative equation is presented.

Introduction

Solid oxide fuel cells (SOFCs) are the most attractive energy generation system because of their efficiency, which is improving every day, and contaminant-free energy generation. Usually, nickel with yttrium stabilized zirconia (Ni–YSZ) cermet is used for the anode, $La_{1-x}Sr_xMnO_3$ for the cathode and YSZ for the electrolyte preparation [1, 2]. Their operation temperature is between 600°C and 1000°C. Any phase transformation produced during the controlled solid state reactions at these temperatures has a big influence in the SOFC's properties and performance. Therefore, the study of the dynamics of these transformations is very important for the possible applications of these devices.

Anode studies for SOFC applications are focused to improve their efficiency using new precursors [3, 4]. This efficiency depends, among other parameters, on the porosity size distribution to maintain the triple phase boundary (TPB), and graphite and some polymers have been used as precursors to obtain such porosity [5,6]. In particular the cermet anode's electrochemical activity depends on the Ni and YSZ ratio [7]. The advantages of this SOFC include the use of gas, such as CO and H_2, as feed without the use of noble metals as catalyst and very low levels of SO_x and NO_x emissions, thus reducing cell costs [8, 9].

Reduction of Ni–YSZ has been already performed by some authors to study kinetics parameters of the reaction with good results. All these studies employed materials with Ni/3 mol% Y_2O_3–ZrO_2 (Ni/Y–TZP) cermet electrodes that were evaluated with galvanostatic current interruption (GCI) and electrochemical impedance spectroscopy (EIS) techniques. However the amount of Y_2O_3 has not worked quite well

in SOFCs [10]. Some authors have used in situ timeresolved X-ray diffraction (TRXRD) to study the NiO powders reduction [11] and calorimetric techniques using redox cycles to study the microstructure of Ni/YSZ bulk ceramics [12]. In this work the phase transformations and dynamics that take place during the NiO–YSZ→Ni–YSZ reduction are analysed. Their structural and chemical characterization during the isothermal reduction were analysed by in situ TRXRD and refined with the Rietveld method, which allowed knowing the kinetic process of the reduction. The microstructure was observed by scanning electron microscopy (SEM) and its chemical compositionwas obtained by x-ray energy dispersive spectroscopy (EDS).

Some works have made quantitative analyses of Ni–YSZ cermet microstructure by optical and SEM techniques to differentiate each phase during reduction, but this was not easy because particle size and backscattered coefficients of the cermet phases are quite similar [13]. Thus, the use of the Rietveld method is proposed in this work in order to avoid these problems. X-ray diffraction (XRD) at high temperatures, together with position sensitive detectors (PSD), is a very suitable complement to conventional thermal analysis (DSC, TGA and TMA). Moreover with the in situ TRXRD analysis we can follow and study the phase transformations and distinguish among different amorphous solid and/or liquid phases, as well as get important information on their kinetics [14].

Experimental

Eight Ni–YSZ cermets with concentrations ranging from 15%wt to 66%wt Ni were prepared using high-purity precursors, nickel acetylacetonate (NiAA) and an Aldrich YSZ (8%mol yttrium) with >99.9% purity (see table 1). The organic content of NiAA in

the sample with 15%wt Ni was used as pore-former in all cermets, which maintains the pore volume constant throughout the sample. To increase the amount of NiO in the samples, an extra amount of Ni was added, until it reached a maximum of 66%. NiAA was calcinated at 800°C to obtain enough NiO to be added to these samples.

The samples were milled in an agate mortar during 1 h, and the obtained powders were afterwards compressed into 1 cm-in-diameter discs with 1mm thickness using a 1-ton unidirectional axial pressure for 5 s, and drying them at 110°C during 24 h. Afterwards, the discs were calcinated from room temperature to 800°C with a heating rate of 1°C min−1 in an atmospheric air-heated box furnace for 2 h. Once the pore was formed, the disc samples were sintered at 1400°C for 2 h with a heating rate of 5°C min_{-1}. The cooling rate for each anode was 5°C min_{-1}.

A special NiO–YSZ sample (sample 9, S9), with 90%wt NiO and 10%wt YSZ (>99.9% purity), was mixed with ethyl alcohol in an agate mortar and a drop was placed on an x-ray powder diffractometer heating holder (model D5000 Siemens, equipped with CuKα monochromatic radiation, θ–θ geometry and with a PSD detector) to carry out the kinetic study by TRXRD at 800°C in a 10% H_2 and 90% N^2 atmosphere, with a flow ≈150 cm^3 min^{-1}. Thus the in situ reduction from NiO–YSZ to Ni–YSZ and time reduction for the cermets were obtained. It is worth commenting that for a kinetic study, the time typically required for collecting an individual diffraction pattern is 20 min, howeverwe decided to obtain them in periods of 8 h each one by using a PSD-50m MBRAUN. Once the TRXRD data were obtained during the isothermal reduction $NiO_{(111)} \rightarrow Ni_{(111)}$, all the patterns were refined with the Rietveld method to quantify the

amount of transformed phase y(t) and to determine the reaction rate. Thus the kinetic data of the solid state crystallization were obtained.

After reduction, each of the 8 sintered discs was reduced in a furnace with 10% H2 in N2 atmosphere at 800°C. For the observation of the microstructure a JEOL-5600 SEM microscope was used. This microscope has attached EDS NORAN equipment.

The Rietveld method

The use of the Rietveld method has been well recognized for calculating structural parameters from neutron and XRD data of almost all types of solid materials (not only single crystals). Intensities y_{ci} are determined from the $|F_K|^2$ values calculated by structural models and they can be related to the 2θ angle [15]. Once the data have been refined and the results converted into the transformed fractions, the reaction rate as a function of time y(t) can be obtained.

Table 1. Expected and calculated concentration and cell volume of Ni and domain size for the cermets. The calculated data were obtained with the Rietveld method as described in the text.

	Samples	S1	S2	S3	S4	S5	S6	S7	S8
Ni (%wt)	Expected	14.2	18.5	22.8	37.2	43.1	51.2	55.3	66.2
	Calculated	15±1	18±1	23±1	34±1	46±1	49±1	56±1	66±1
	Difference	−5.6	2.7	−0.9	8.6	−6.7	4.3	−1.3	0.3
Domain size (nm)	Ni [(c)]	>1000	>1000	>1000	>1000	>1000	>1000	>1000	>1000
	YSZ [(c)]	122(3)	120(3)	127(2)	128(2)	123(3)	124(1)	125(1)	126(2)
	YSZ [(t)]	302(5)	305(4)	297(6)	291(5)	304(3)	306(5)	293(5)	289(6)
Cell volume (Å^3)	Ni	43.834(3)	43.829(3)	43.814(1)	43.804(3)	43.796(2)	43.785(3)	43.781(2)	43.755(1)

[(c)] Cubic phase, [(t)] tetragonal phase. The number in parentheses is the error of the last number.

Intensities $y_{ci}(2\theta)$ are determined from the values calculated by F_K structural models with the following relation [3]:

$$y_{ci} = s \cdot \sum_m L_m |F_m|^2 \phi\,(2\theta_i - 2\theta_m)\, P_m \cdot A + y_{bi}, \qquad (1)$$

where s is the scale factor, m indicates the corresponding Miller indices, L_m the Lorentzian polarization and multiplicity factors, φ the reflection profile function, P_m the

preferred orientation function, A an absorption factor, F_m the structure factor and y_{bi} is the background intensity at the ith step.

Kinetic parameters such as concentration y(t) are measured from XRD data with the following expressions [14]:

$$y_\alpha(t) = 1 - \frac{I_\alpha(t) \cdot [K_2(\alpha) - I_\alpha(0) \cdot (\mu_\alpha - \mu_\beta)]}{I_\alpha(0) \cdot [K_2(\alpha) - I_\alpha(t) \cdot (\mu_\alpha - \mu_\beta)]} \quad (2)$$

for the α fraction and

$$y_\beta(t) = 1 - \frac{I_\beta(t) \cdot [K_2(\beta) - I_\beta(\infty) \cdot (\mu_\beta - \mu_\alpha)]}{I_\beta(\infty) \cdot [K_2(\beta) - I_\beta(t) \cdot (\mu_\beta - \mu_\alpha)]} \quad (3)$$

for the β fraction. Here K_2 is a constant and μ_α and μ_β are the linear absorption coefficients of the α and β components, respectively.

y(t) was calculated by the Rietveld method and the reaction rate can be determined through the following relations:

$$y_\alpha(t) = 1 - \frac{C_\alpha(t)}{C_\alpha(0)}, \quad (4)$$

$$y_\beta(t) = \frac{C_\beta(t)}{C_\beta(\infty)}, \quad (5)$$

where α and β are the fraction consumed and formed at any time t , respectively.

The crystallographic density ρc was calculated from the volume data obtained by the Rietveld analysis; and then used to calculate porosity (p) according to the following equation:

$$p = 1 - \left(\frac{\rho}{\rho_c}\right), \quad (6)$$

where ρ is the bulk density.

Structure data refinements by the Rietveld method from the 8 samples were collected before and after the reduction process, using a 2θ angle range from 20° to 80° with 0.02° step size and 10 s step^{-1}. Structure parameters were obtained using the Rietveld method with the FULLPROF program [16], and a peak shape modified Thompson–Cox–Hasting pseudo-Voigt function for the calculated reflection profile. The reproducibility for the (a) background parameters, (b) scale factors, (c) instrumental effects (zero-point and sample offcentring), (d) structural parameters, (e) profile parameters, (f) domain size parameters and (g) phase quantification was considered for refinement until the results converged into minimum values. Instrumental broadening U, V and W were determined from the Rietveld refinement of an Al_2O_3 powder sample XRD pattern (a standard for quantitative analysis in XRD) [17], and the results were used in the refinement of all patterns. Their calculated values were U = 0.019 11,V = −0.028 281 and W = 0.011 999. Domain size (crystal size) determination was done by considering the Bragg reflection profile broadening [18]. All data for the crystallographic study were obtained from well known references [19–24].

Results and discussion

Microstructure and porosity:

The percentage of Ni in each of the 8 samples is indicated in table 1 together with the one calculated with the Rietveld method and the domain size of the cermets. Some differences were observed for the average domain size of YSZ crystals. Domain size for the YSZ cubic phase was 125 nm, whereas it was almost twice that for the tetragonal phase at 300 nm (see table 1).

Anode porositywas found to be proportional to the amount of Ni in the sample. This can be explained by the volume size change during the reduction process. In order to optimize the TPB, it was suggested that the porosity of the SOFCs' anodes must be of around 40%. In the sample of 46%wt Ni (sample S5) porosity close to this value was obtained. Incidentally, a content of 45%wt Ni reduces the difference in the thermal expansion coefficient between the two phases [13].

It should be emphasized that calcination was carried out at 1°C min^{-1}, in order to avoid any cermet fracture. The microstructure of all the cermets observed with SEM before and after the reduction process was very similar. In figure 1 the microstructure of the anode with 46%wt Ni is shown. TheSEM analysis showed that the cermets had the same morphology and an average YSZ particle size of 0.5m approximately. Particles of YSZ, which were analysed with EDS, were observed surrounding the particles of NiO. These NiO particles have sizes from 1 to 4μm.

XRD analysis:

Figure 2 shows a plot of the relative intensity versus diffraction angle for the isothermal reduction NiO–YSZ → Ni–YSZ at 800°C (sample S9). An intensity decrement occurs for the plane $(111)_{NiO}$, whereas a symmetrical and simultaneous increment is observed for the plane $(111)_{Ni}$ during the first 40 min. Subsequently, for the next 8 h, the intensity of the plane $(111)_{NiO}$ continuously decreases but at a very slow rate. The intensity of the plane $(111)_{Ni}$ seems to increase at the same rate (figure 3).

Similar behaviour was observed in other works [10] when NiO was reduced at temperatures lower than 800°C but the maximum reducing rate is much smaller than the one obtained here. High and low profile reduction can be produced by the content of

YSZ, and by the fact that they surround the NiO particles as it does not happen when single NiO particles are reduced [10]. Thus the reduction process is obstructed.

Rietveld analysis:

The results with the Rietveld method for the cermets (discs) were obtained using the space group $Fm\bar{3}m$ for the YSZ cubic phase, $P4_2/nmc$ for the YSZ tetragonal phase and $Fm\bar{3}m$ for the NiO and Ni cubic unit cells. The possible presence of the cubic and tetragonal phases of YSZ (8%mol) was observed in the eight cermets (Ni–YSZ) after reduction. As an example, figure 4 shows the final cermet fitting with 56% Ni (sample S7) calculated before (figure 4(a)) and after (figure 4(b)) reduction.

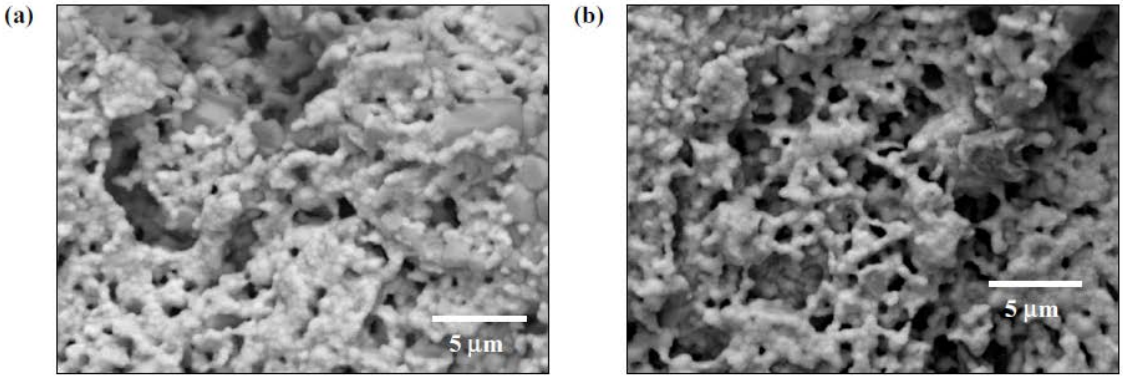

Figure 1. SEM images of sample S5 cermets composite sintered at 1400°C for 2 h in air. Before (*a*) and after (*b*) reduction process.

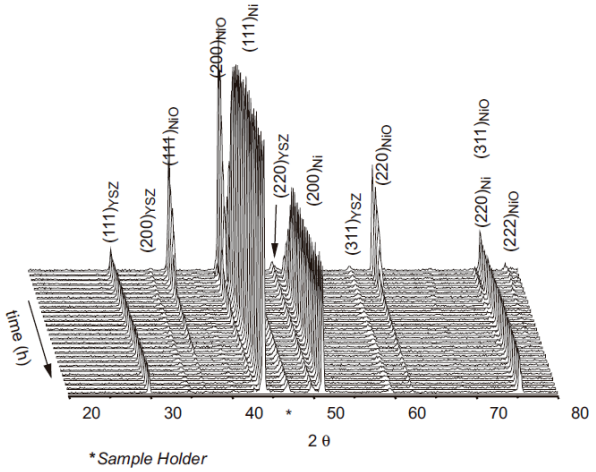

Figure 2. Time-resolved XRD for the isothermal reduction NiO–YSZ → Ni–YSZ at 800°C under N–H_2 atmosphere (sample S9). The peak labelled with (*) corresponds to the sample holder.

The experimental profile is indicated by (+), then calculated by (−) and the difference plot between the observed and calculated intensities is shown in each case. All the samples showed similar behaviour. In these figures, an acceptable adjustment for the differences between the observed and calculated profile intensities was registered. In the insert of figure 4(b) an amplification of the region between 70° and 78° is presented. Here the planes $(004)_t$ and $(220)_t$ confirm the presence of the YSZ tetragonal phase whereas the plane $(400)c^*$ indicates the presence of the YSZ cubic phase. As is observed in figure 6, almost flat differences were obtained between the observed and calculated profile intensities. Adjustment degree for fitting patterns was from 5 to 10 (R_{wp}).

Crystal structure data for Ni obtained with *in situ* Rietveld analysis during the reduction process showed some slight change in volume. Figure 5 shows a decrement in the cubic unit cell volume as a function of the Ni content after the reduction process. Cell volumes of Ni structures from 44.17Å^3 [25] to 43.76Å^3 [26], have been obtained by other authors. These values are close to those for 15%Ni and 66%Ni. The cermets showed this behaviour when the ratio c/t decreased and Ni% increased.

An important result obtained in this work is related to the YSZ cubic to tetragonal phase ratio (c/t). Figure 6 shows the variation of the c/t ratio as a function of the Ni content: as the Ni content increases, c/t decreases reaching a limiting value around 1.07. However, the YSZ tetragonal phase increased around a tenth with respect to the cubic phase when the Ni concentration increased. The unit cell parameters (a, b, c) for both YSZ phases remain unchanged after the reduction process.

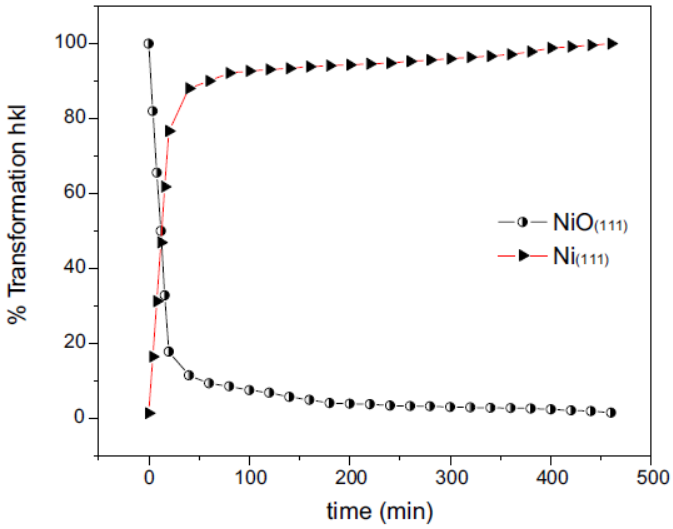

Figure 3. Transformation relationship between $NiO_{(111)} \rightarrow Ni_{(111)}$ during the reduction process (sample S9).

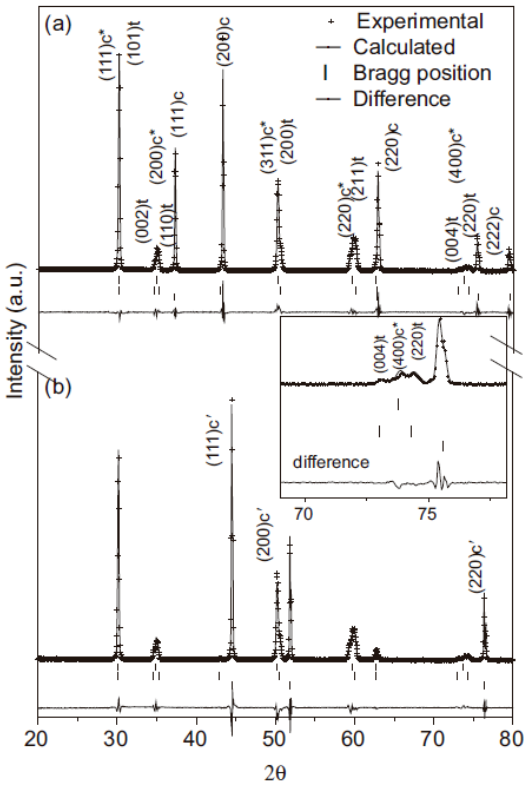

Figure 4. Example of the experimental and calculated XRD pattern by the Rietveld method before reduction (*a*) and after reduction (*b*) for sample 7. The insert in (*b*) shows an amplification of the region between 70° and 78°. Planes $(004)_t$ and $(220)_t$ confirm the presence of the YSZ tetragonal phase, whereas the plane $(400)c^*$ indicates the presence of the YSZ cubic phase. C represents the cubic structure of NiO and C′ the cubic structure of Ni.

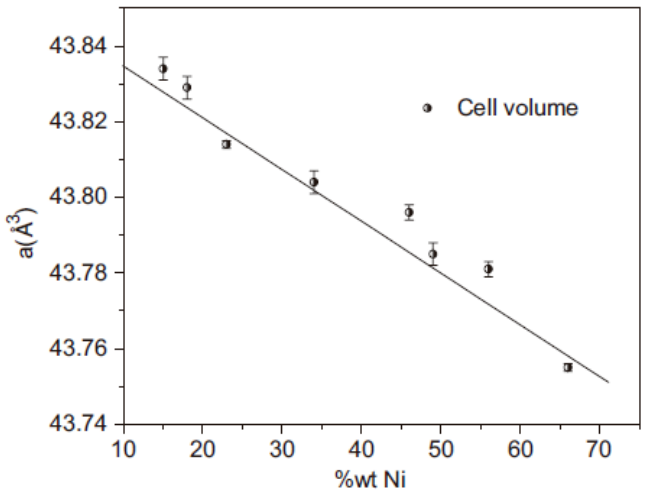

Figure 5. Cell volume (in per cent) as a function of the Ni content of samples after reduction calculated by the Rietveld method. The concentration of tetragonal phase in the cermets could be responsible of this behaviour.

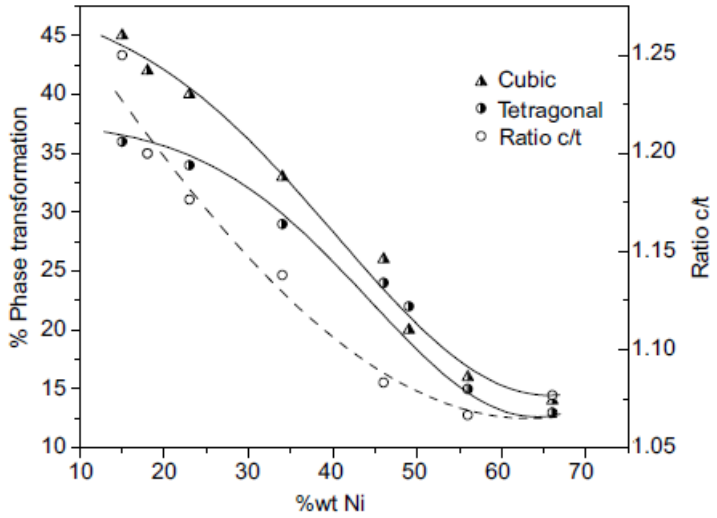

Figure 6. YSZ cubic to tetragonal ratio c/t and percentage phase variation as a function of the %Ni content of samples. Note that c/t decreases as the Ni content increases, reaching a limiting value around 1.07.

Kinetic analysis:

Sometimes the crystallization process is described by the Johnson–Mehl–Avrami (JMA) equation:

$$f = 1 - \exp(-Kt^n), \qquad (7)$$

which relates the volume fraction of transformed material, f , to the reaction time, t . Here K is the characteristic nucleation process quotient (whether the nuclei interfere with one another, or they are nucleated independently) and n is the characteristic nuclei shape coefficient (e.g. for spherical nuclei, n = 4).

The experimental fractional data $C(t)/C_{max}$ obtained from TRXRD is shown in figure 7. Equation (7) was tested with this experimental data resulting in a poor fit since this equation considers only a single type of process, whereas our experimental data exhibits two regions. Figure 7 also shows the experimental data fitted with a continuous curve that was obtained assuming a rate expression that accounts for a reaction order shift [27]:

$$\frac{dC}{dt} = \frac{k_1}{1 + k_2 C^n}. \qquad (8)$$

Equation (8) considers that the reaction behaves differently when there is an excess of one of the phases, being almost of zeroth order for the low conversion region ($k_2C^n << 1$), with a rate constant of $k_1 = 3.9$. When there is an excess of the final product, the reaction becomes inversely proportional to some power of the concentration (n = 14.56), with a rate constant of $k1/k2 = 1.926 \times 10^{-27}$. As can be seen in figure 7, the fitting with equation (8), is quite good. In figure 4 are also shown the straight lines that best fit each of the regions separately. The first region extends up to a conversion of approximately 82%.

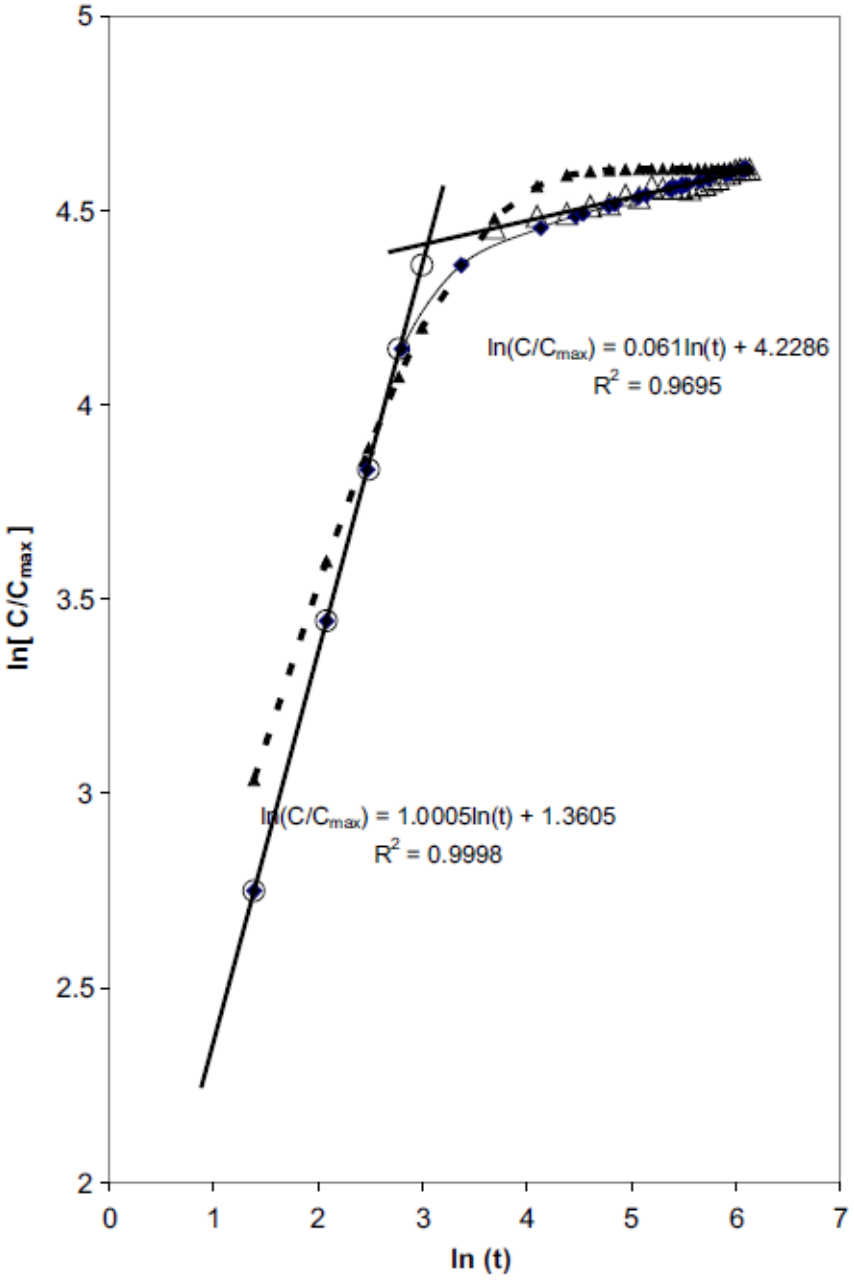

Figure 7. Kinetic data from the TRXRD analysis of phase transformation NiO–YSZ → Ni–YSZ at 800°C. The dashed curve was obtained with equation (7), whereas the continuous curve was with equation (8). Markers are experimental (%wt) data points calculated with the Rietveld method (sample S9).

Conclusions

A kinetic study by in situ TRXRD of cermet reduction (NiO– YSZ→Ni–YSZ) at atmospheric pressure and 800°C, revealed a transition from a high to a low reduction rate. All the process appears to be kinetically controlled with a change in the reaction order as the reaction proceeds. The volume of YSZ remains unchanged during both sintering and reduction. A decrease of cell volume of the nickel cubic structure was found when the Ni content increased. Crystal structure data show that as the Ni content increases, the ratio c/t decreases, reaching a limiting value. These results can be explained by the presence of tetragonal phase in Ni–YSZ 8%mol and the amount of Ni after sintering at 1400°C for 2 h and reduction to 800°C with H_2–N_2 atmosphere for 8 h. Equation (8) fits quite well with the experimental results obtained in this work because it considers that the reaction behaves differently where there is an excess of one of the phases.

Acknowledgments

The authors would like to thank Victor Hugo Ramos Sánchez and D Lardizábal for their valuable participation in this work. We would also like to thank the Universidad Autónoma del Estado de México, Facultad de Química and Centro de Investigación en Materiales Avanzados SC for the facilities provided for this work.

References

[1] Carrillo A S, Tagawa T and Goto S 2001 Mater. Res. Bull. 36 1017–27

[2] Yoona S P, Hana J, Nama SW, Lima T H, Oha I H, Honga S A, Yoob Y S and Limb H C 2002 J. Power Sources 106 160–6

[3] Lu Z, Pei L, He T M, Huang X G, Liu Z G, Yuan Ji Y and

Su W H 2002 J. Alloys Compounds 334 299–303

[4] Dongare M K, Dongare A M, Tare V B and Kemnitz E 2002 Solid State Ion. 152–153 455–62

[5] Jang W S and Hyun S H 2002 J. Mater. Sci. 37 2535–41

[6] Kim J H, Song R H, Song K S, Hyun S H, Shin D R and Yokokawa H 2003 J. Power Sources 122 138–43

[7] Ko J H, Yoo Y S, Park J and Lim H C 2002 Solid State Ion. 149 157–66

[8] Fuku T and Ohara S 2001 Japan. J. Chem. Eng. 34 964–6

[9] Singhal S C 2002 Solid State Ion. 152–153 405–10

[10] Jiang S P and Ramprakash Y 1999 Solid State Ion. 122 211–22

[11] Rodriguez J A, Hanson J C, Frenkel A I, Kim J Y and Perez M 2002 J. Am. Chem. Soc. 124 346–51

[12] Fouquet D, Muller A C, Weber A and Ivers Tiffee E I 2002 Proc. European Solid Oxide Fuel Cell Forum pp 467–74

[13] Lee J H, Moon H, Lee H W, Kim J, Kim D D and Yoon K H 2002 Solid State Ion. 148 15–26

[14] Chung D D L 1993 X-Ray Diffraction at Elevated Temperatures: A Method For In-situ Process Analysis (New York: VCH) pp 237–49

[15] Young R A (ed) 1993 The Rietveld Method School of Physics, Georgia Institute of Technology, Atlanta

[16] Rodriguez-Carvajal J 1998 Program Fullprof 98 version 0.2,

Laboratorie Leon Brillouin (CEA-CNRS)

[17] National Institute of Standards and Technology 1989 Standard Reference Material 674a, Department of Commerce, United States of America

[18] Gualtieri A F 2000 J. Appl. Crystall. 33 267–78

[19] JCPDS—International Centre for Diffraction Data Copyright (C) JCPDS-ICDD 2000, card 04-0835

[20] JCPDS—International Centre for Diffraction Data Copyright (C) JCPDS-ICDD 2000, card 30-1468

[21] JCPDS—International Centre for Diffraction Data Copyright (C) JCPDS-ICDD 2000, card 04-0850

[22] JCPDS—International Centre for Diffraction Data Copyright (C) JCPDS-ICDD 2000, card 42-1164

[23] Inorganic Crystal Structure Database ICSD version 2004-1 (atomic positions)

[24] International Tables for Crystallography 1996

[25] Yousuf M, Sahu P C, Jajoo H K, Rajagopalan S and Govinda Rajan K 1986 J. Phys. F: Met. Phys. 16 373–80

[26] Swanson H E and Tatge E 1967 Acta Crystallogr. 1 1948–23

Swanson H E and Tatge E 1954 Acta Crystallogr. 7 464

[27] Levenspiel O 1999 Chemical Reaction Engineering 3rd edn (New York: Wiley)